

# Thermoelectric properties of topological chains coupled to a quantum dot

A. C. P. Lima<sup>1</sup>, R. C. Bento Ribeiro<sup>1</sup>, J. H. Correa<sup>2</sup>, Fernanda Deus<sup>3</sup>, M. S. Figueira<sup>4</sup>, and Mucio A. Continentino<sup>1\*</sup>

<sup>1</sup> Centro Brasileiro de Pesquisas Físicas, Rua Dr. Xavier Sigaud,  
150, Urca 22290-180, Rio de Janeiro, RJ, Brazil

<sup>2</sup> Universidad Tecnológica Del Perú, Nathaliao Sanchez, 125, Lima, Perú

<sup>3</sup> Universidade do Estado do Rio de Janeiro, Faculdade de Tecnologia,  
Departamento de Matemática, Física e Computação,  
Rodovia Presidente Dutra km 298, 27537-000, Resende, RJ, Brazil and

<sup>4</sup> Instituto de Física, Universidade Federal Fluminense,  
Av. Litorânea s/N, CEP: 24210-340, Niterói, RJ, Brasil

Topological one-dimensional superconductors can sustain in their extremities zero energy modes that are protected by different kinds of symmetries. The observation of these excitations in the form of Majorana fermions is one of the most intensive quests in condensed matter physics. Their study is not only interesting in itself, but also because they have promising applications in the area of quantum computation. In this work we are interested in another class of one dimensional topological systems, namely topological insulators. These also present symmetry protected end modes with robust properties and do not require the low temperatures necessary for topological superconductivity. We consider the simplest kind of topological insulators, namely chains of atoms with hybridized *sp* orbitals. We study the transport properties of these chains in the trivial, non-trivial topological phases and at the quantum topological transition. We use a simple device consisting of two semi-infinite hybridized *sp*-chains connected to a quantum dot and obtain the thermoelectric properties of this system as a function of temperature and distance to the topological transition. We show that the electrical conductance and the Wiedemann-Franz ratio of the device at the topological transition have universal values at very low temperatures. The thermopower gives direct evidence of fractional charges in these systems.

## I. INTRODUCTION

The study of topological systems is now one of the most active areas of research in condensed matter physics [1, 2]. The theoretical efforts to understand the properties of these systems has lead to the predictions of emergent excitations with unexpected properties that make them potentially useful for different types of applications. Among these theoretical works, Kitaev model for a *p*-wave superconducting chain [3] has played a fundamental role and many suggestions have appeared of how to realize this model in actual physical systems. In the topological phase, the finite one-dimensional Kitaev superconducting chain presents Majorana, zero energy modes, at its ends. The physical implementation of the *p*-wave Kitaev model and the detection [4] of the zero energy Majorana modes is a modern Graal in materials research. In this pursuit an initial major difficulty is to obtain a *p*-wave superconductor, since this is far from being common in nature [5]. Several proposals have been put forward to generate this type of pairing in a chain, mostly using proximity effects and magnetic fields.

Besides one-dimensional *p*-wave superconductors there is a class of topological insulating [6, 7] chains that is much simpler and also presents protected zero energy modes at their ends. A representative member of this class are *sp*-chains consisting of atoms with hybridized *s* and *p* orbitals [8]. The mixing between *s* and *p* orbitals in neighboring ions is antisymmetric and this gives rise to non-trivial topological properties [9], in close analogy with the antisymmetric *p*-wave paring of the Kitaev chain. Notice that the asymmetry of the mixing holds for any pairs of orbitals that have angular momentum quantum numbers differing by an odd number. There is another class of *sp*-chains with intra-atomic *sp* hybridization that also presents topological phases. As we show, this maps into the well-known, topologically non-trivial, Su-Schrieffer-Heeger (SSH) model [10]. The *sp*-chains may be easier to realize in practice than *p*-wave superconductors. Also they do not require the low temperatures necessary for superconductivity to manifest their topological properties.

A possible realization of the *sp*-chain is carbyne [11–15], the one-dimensional allotropic form of carbon. In this system the 2*s* orbital hybridizes with a *single* 2*p* orbital favoring a linear atomic alignment. A significant effort has been made in the synthesis of these materials that in principal can exist in a metallic state (cumulene) and in an insulating, broken symmetry state, with alternating single and triple bonds [12].

\* corresponding author:muciocontinentino@gmail.com

In spite of the symmetry protection of the edge modes in topological *sp*-chains, these modes have distinct features from the Majoranas in the Kitaev chain. The former are quasi-particles with a hybrid *sp*-character that are formed of two different types of Majoranas [8]. In this paper we study the properties of the edge modes in topological *sp*-chains. We consider a simple device consisting of two identical semi-infinite *sp*-chains connected to a quantum dot. We obtain the electrical and thermal transport properties of this system as a function of temperature in the topologically non-trivial and trivial phases, and at the topological transition of the chains. The edge modes determine the low temperature transport properties of the device since the bulk of the chains is insulating in both trivial and non-trivial topological phases.

The *surface* density of states of the chain is obtained using a Greens functions approach [8, 16]. This provides direct information on the topological phase of the chain and establishes a form of bulk-boundary correspondence, since it can be obtained from properties of the bulk.

## II. TWO TYPES OF TOPOLOGICAL CHAINS

### II.1. The inter-atomic *sp*-chain

We start with, possibly, the most simple case of a topological insulator. This is a non-interacting atomic chain with two orbitals per site. The fundamental point is that these orbitals have different parities, such that the hybridization between them, in neighboring sites, is antisymmetric, i.e.,  $V_{ij} = -V_{ji}$ . The simplest realization of this system is the inter-atomic *sp*-chain. The Hamiltonian describing this system is given by [8, 16],

$$\begin{aligned} \mathcal{H}_{sp} = & \epsilon_s^0 \sum_j c_j^\dagger c_j + \epsilon_p^0 \sum_j p_j^\dagger p_j - \sum_j t_s (c_j^\dagger c_{j+1} + c_{j+1}^\dagger c_j) + \sum_j t_p (p_j^\dagger p_{j+1} + p_{j+1}^\dagger p_j) \\ & + V \sum_j (c_j^\dagger p_{j+1} - c_{j+1}^\dagger p_j) - V^* \sum_j (p_j^\dagger c_{j+1} - p_{j+1}^\dagger c_j) \end{aligned} \quad (1)$$

where  $\epsilon_{s,p}^0$  are the centers of the *s* and *p* bands, respectively. The  $t_{s,p}$  represent the hopping of *spinless* electrons to neighboring sites in the same orbital and  $V$  the antisymmetric hybridization between *s* and *p* states in neighboring sites. Due to the different parities of the orbital states, this hybridization is odd-parity, such that, in momentum space  $V(-k) = -V(k)$ . Then the mixing term breaks the parity symmetry of the system in spite that the chain is centro-symmetric. Notice that the spin-orbit coupling (SOC) also breaks parity symmetry [17], but differently from hybridization that mixes quasi-particles with the same spin, SOC mixes quasi-particles with opposite spins [17]. For simplicity we consider here the case of spinless fermions and take the chemical potential  $\mu = 0$ .

The energy of the quasi-particles of the infinite chain can be easily obtained using, for example, the Green's function method [8]. The excitations are obtained from the poles of the Green's function that occur at

$$(\omega - \epsilon_s^0 + 2t_s \cos ka)(\omega - \epsilon_p^0 - 2t_p \cos ka) - 4V^2 \sin^2 ka = 0. \quad (2)$$

We considerer symmetric bands, such that,  $\epsilon_s^0 = -\epsilon_p^0 = \epsilon$ . Furthermore, we assume  $t_s = t_p = t$ . In this case the energy of the quasi-particles is given by,

$$\omega_{1,2}(k) = \pm \sqrt{(\epsilon - 2t \cos ka)^2 - 4V^2 \sin^2 ka}. \quad (3)$$

The two quasi-particle bands are generally separated by a gap and for  $\mu = 0$  the system is an insulator. However, for  $\epsilon/2t = 1$  the system becomes gapless at  $k = 0$ . For  $\epsilon/2t > 1$ , the chain is a band insulator with a gap between the valence and conduction bands. For  $\epsilon/2t < 1$ , there is a band inversion, the system is still an insulator, in fact a topological insulator [8]. Then, at  $\epsilon/2t = 1$  a topological quantum phase transition takes place. The excitations at the quantum critical point (QCP) are Dirac-like fermions with a linear dispersion relation. The characterization of the topological nature of the insulating phases, for different values of  $\epsilon/2t \neq 1$ , requires the calculation of a topological invariant [8]. This takes different values in these phases, according to their trivial or non-trivial topological character. A finite chain in its topological non-trivial phase has edge states that are protected by the symmetries of the Hamiltonian. The zero energy modes can be obtained rewriting the *sp* Hamiltonian, Eq 1 in terms of Majorana operators [8]. At each end of the chain there is *one pair* of Majorana modes that correspond to a quasi-particle with hybrid *s* and *p* character.

In this work, to show the existence of the edge modes in the non-trivial topological phase, we follow a different approach that consists in calculating the density of states at the end of a semi-infinite *sp*-chain. This method was introduced earlier [18], but no connection was made with the topological character of the chain. It consists in

considering the surface of the semi-infinite chain as a defect and treating it using a scattering approach. The frequency dependent Green's function  $G_{00}$  at the edge of the semi-infinite chain can be obtained as [18],

$$G_{00}(\omega) = \frac{1}{\omega} \left[ \tilde{\omega}^2 - \tilde{\epsilon}^2 + 1 \pm \sqrt{(\tilde{\omega}^2 - \tilde{\epsilon}^2 + 1)^2 - 4\tilde{\omega}^2} \right] \quad (4)$$

where, for simplicity, we take  $\epsilon_s^0 = -\epsilon_p^0 = \epsilon$ ,  $t_s = t_p = V = t$  and define  $\tilde{\omega} = \omega/2t$  and  $\tilde{\epsilon} = \epsilon/2t$ . The density of states at the edge of the chain is given by

$$\rho(\omega) = \frac{-1}{\pi} \text{Im}G_{00}(\omega), \quad (5)$$

and the total number of particles per volume

$$n = \frac{-1}{\pi} \int d\tilde{\omega} \text{Im}G_{00}(\tilde{\omega}). \quad (6)$$

For two full bands of spinless fermions we have,  $n = 2$ .

## II.2. The intra-atomic *sp* chain

We can consider another type of *sp*-chain with intra-atomic hybridized *sp*-orbitals where the quasi-particles can hop to neighboring sites in the chain [19]. The model also describes a mono-atomic carbon chain, like in the case of polyene carbyne [13], with single and triple alternating bonds. This chain maps into a well-known system, namely the SSH chain introduced as a model for polyacetylene [6]. This is another remarkable case of a topological, one dimensional non-interacting system. The model consists of a chain with alternating hopping terms that in the case of carbyne correspond to single and triple bonds,

$$\mathcal{H} = - \sum_n V_1 (|n\rangle\langle\tilde{n}| + |\tilde{n}\rangle\langle n|) - V_2 \sum_n (\widetilde{|n\rangle\langle n+1|} + |n+1\rangle\langle\tilde{n}|), \quad (7)$$

where  $V_1$  and  $V_2$  are hopping terms that alternate along the chain. For a semi-infinite chain the sum extends from  $n = 0$  to  $n = \infty$ . The symbol tilde distinguishes sites in different sub-lattices. For the *sp*-chain [19], the term  $V_1$  corresponds to an intra-atomic *hopping* connecting bonding and anti-bonding states resulting from mixed *sp*-states in a given atom and  $V_2$  to the hopping of a quasi-particle from one atom to another.

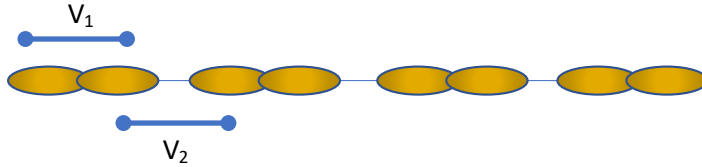


FIG. (1) (Color online) A mono-atomic chain with intra-atomic *sp*-hybridized orbitals and nearest neighbor hopping  $V_2$ . In this case  $V_1$  is the splitting between the two *sp* orbitals. This chain can also be seen as a model for carbyne in the polyene phase where  $V_1$  and  $V_2$  represent single and triple bonds [13]. Notice that the topological transition at  $V_1 = V_2$  occurs between two insulating states.

In order to obtain the surface density of states of the semi-infinite SSH chain, we use a different method, much simpler than the scattering approach. It was developed in Ref. [20] to calculate the local Green's functions at the edge of a semi-infinite chain. The local Green's function of the edge of the SSH-chain is given by

$$G_{00}(\omega) = \begin{pmatrix} \omega & V_1 & 0 \\ V_1 & \omega & V_2 \\ 0 & V_2 & G_{00}^{-1} \end{pmatrix}_{(00)}^{-1} \quad (8)$$

where the label refers to the first matrix element. Inverting the matrix, we arrive at a self-consistency problem involving a second degree algebraic equation

$$[V_2 G_{00}]^2 - 2\alpha[V_2 G_{00}] + 1 = 0, \quad (9)$$

with

$$\alpha(\omega) = \frac{\omega^2 + V_2^2 - V_1^2}{2V_2\omega}. \quad (10)$$

The surface local Green's function is given by

$$G_{00}(\omega) = \frac{1}{2\omega} \left[ \tilde{\omega}^2 - \tilde{V}^2 + 1 \pm \sqrt{(\tilde{\omega}^2 - \tilde{V}^2 + 1)^2 - 4\tilde{\omega}^2} \right] \quad (11)$$

where  $\tilde{\omega} = \omega/V_2$ , and  $\tilde{V} = V_1/V_2$ . The *surface* density of states and the total number of particles per volume are given by Eqs. 5 and 6, respectively with  $n = 1$ . Notice that the local Green's functions, Eqs. 4 and 11 differ only by a factor 1/2 and the energy renormalization factors. Also the integrals in frequency like in Eq. 6 are identical in both cases. The factor (1/2) appears just in the case of the inter-atomic *sp*-chain because it has two orbitals per site.

The topological properties of the finite SSH chain are well-known [6]. It has a topological phase, with two protected edge states for  $V_1/V_2 < 1$ . For,  $\tilde{V} = V_1/V_2 > 1$  this chain is topologically trivial and has no edge modes. The topological transition occurs for  $\tilde{V} = 1$  and is associated with the closing of a gap in the dispersion relation of the infinite chain.

### III. THE SURFACE DENSITY OF STATES

In this section we look in detail at the surface density of states of the semi-infinite *sp*-chain. Since in terms of the renormalized energies the results are very similar for both intra and inter *sp*-chains, as can be seen from Eqs. 4 and 11, we will concentrate in the former, or equivalently in the SSH-chain. In this case the surface density of states is given by

$$\rho(\omega) = \frac{-1}{\pi} \text{Im} \left\{ \frac{1}{2V_2\tilde{\omega}} \left[ \tilde{\omega}^2 - \tilde{V}^2 + 1 \pm \sqrt{(\tilde{\omega}^2 - \tilde{V}^2 + 1)^2 - 4\tilde{\omega}^2} \right] \right\} \quad (12)$$

where  $\tilde{\omega} \rightarrow \tilde{\omega} + i\epsilon$ . The sign of the root is chosen so that the density of states is positive and from now on we take  $V_2 = 1$ . This expression can be rewritten as

$$\rho(\omega) = \frac{1}{2} \left\{ D\delta(\tilde{\omega}) + \frac{1}{\pi} \text{Im} \left[ \frac{\sqrt{(\tilde{\omega}^2 + D)^2 - 4\tilde{\omega}^2}}{\tilde{\omega}} \right] \right\}. \quad (13)$$

where  $D = 1 - \tilde{V}^2$ . There is an additional contribution to the zero energy mode due to the second, square root term. Considering this explicitly, we can rewrite Eq. 13 as

$$\rho(\omega) = \frac{1}{2} \left\{ (D + |D|)\delta(\tilde{\omega}) + \frac{1}{\pi} \frac{\text{Im} \sqrt{(\tilde{\omega}^2 + D)^2 - 4\tilde{\omega}^2}}{\tilde{\omega}} \right\}, \quad (14)$$

where one sees that the zero energy mode only appears for  $D > 0$ , or  $\tilde{V} < 1$ , i.e., in the topological phase of the chain (see Fig. 2). In the trivial phase there is a cancellation and the zero energy surface mode disappears. Notice that for  $D > 0$  the zero energy mode is a true surface state since its energy does not coincide with any of the bulk states.

For completeness and since it will be used further on, we also obtain the real part of the surface Green's function (see Fig. 2). This is given by

$$\text{Re}G_{00}(\tilde{\omega}) = \frac{1}{2} \left[ D \frac{1}{\tilde{\omega}} + \tilde{\omega} + \frac{\text{Re} \sqrt{(\tilde{\omega}^2 + D)^2 - 4\tilde{\omega}^2}}{\tilde{\omega}} \right]. \quad (15)$$

Notice that

$$\lim_{\tilde{\omega} \rightarrow 0} \text{Re}G_{00}(\tilde{\omega}) = \frac{1}{2} \frac{(D + |D|)}{\tilde{\omega}}.$$

Then, the local surface Green's function gives direct information on the topological state of the chain. Furthermore, the weight of the zero energy mode vanishes linearly with the distance to the topological transition ( $D \propto (1 - \tilde{V})$ ).

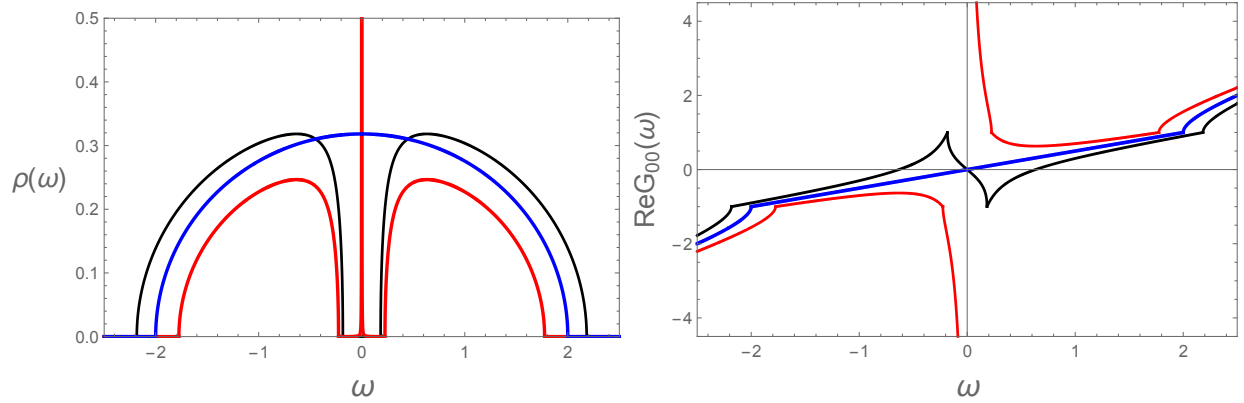


FIG. (2) (Color online) Density of states at the surface of the semi-infinite SSH chain (left panel) and real part of the surface Green's function (right panel) in the topological phase (red), the trivial phase (black) and at the topological transition (blue).

#### IV. CONDUCTANCE OF TWO SEMI-INFINITE CHAINS COUPLED TO A QUANTUM DOT

In this section we introduce a simple device consisting of two identical semi-infinite chains coupled to a quantum dot [21], as shown in Fig. 3. We consider the case of a non-interacting quantum dot with a single state with energy  $E_0$ . The coupling of the chains to the dot is given by a hopping term  $t_d$  that transfers quasi-particles from the chains in and out of the dot, as shown in Fig. 3. The dot yields a connection between the semi-infinite chains and together they allow to probe the nature of the edge states through their contribution to the thermal and electrical conductances of the device, as we discuss below. The local Green's function of the dot connecting the two semi-infinite  $sp$ -chains is given by [21],

$$G_d(\omega) = \frac{g_d}{1 - 2|t_d|^2 g_d G_{00}} \quad (16)$$

where,

$$g_d = \frac{1}{\omega - E_0}$$

is the Green's function of the non-interacting dot. The Green's function  $G_{00}$  is that of the edge of the chains and is given by Eq. 11. Notice that Eq. 16 can be rewritten as,

$$G_d(\omega) = \frac{1}{\omega - E_0 - 2|t_d|^2 \text{Re}G_{00} - i2|t_d|^2 \text{Im}G_{00}}. \quad (17)$$

The dimensionless conductance of the device,  $sp$ -chain-dot- $sp$ -chain can be obtained as in Ref. [22]. It is given by,

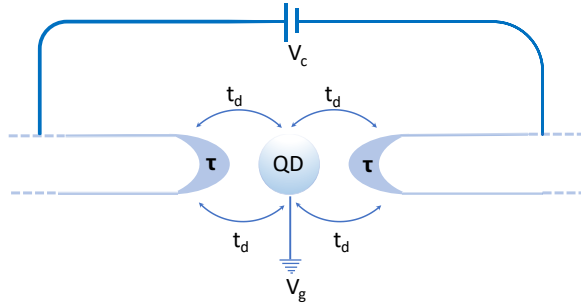


FIG. (3) (Color online) Two semi-infinite  $sp$ -chains connected to a quantum dot (QD). A very small potential difference  $V_c$  is applied in the chains. Notice that  $t_d$  is the coupling between the dot and the chains.

$$G/G_0 = \int d\omega \left( -\frac{\partial f}{\partial \omega} \right) \mathcal{T}(\omega) \quad (18)$$

where  $f(\omega)$  is the Fermi-Dirac distribution and

$$\mathcal{T}(\omega) = -\Gamma \text{Im}G_d(\omega)$$

with  $\Gamma = 2\pi|t_d|^2 \sum_k \delta(\omega - \epsilon_k)$ , the *Anderson broadening* [22]. In Eq. 18,  $G_0 = e^2/\hbar$  is the quantum of conductance.

More generally, we define the quantities,

$$\mathcal{L}_n = \frac{1}{\hbar} \int d\omega \left( -\frac{\partial f}{\partial \omega} \right) \omega^n \mathcal{T}(\omega), \quad (19)$$

in terms of which we can obtain the thermoelectric coefficients. The conductance can be rewritten as  $G = e^2 \mathcal{L}_0$ . The thermal conductance  $K$  and the thermopower  $S$  are given, respectively, by

$$K = \frac{1}{T} \left( \mathcal{L}_2 - \frac{\mathcal{L}_1^2}{\mathcal{L}_0} \right), \quad (20)$$

$$S = - \left( \frac{1}{eT} \right) \frac{\mathcal{L}_1}{\mathcal{L}_0}. \quad (21)$$

These in turn define the ratios corresponding to the Wiedemann-Franz law (WF) and the dimensionless *figure of merit*  $ZT$  that are given, respectively, by

$$WF = \frac{1}{T} \left( \frac{K}{G} \right), \quad (22)$$

$$ZT = \frac{S^2 GT}{K}, \quad (23)$$

where the former ratio WF is given in units of the Lorenz number  $L_0 = (\pi^2/3)(k_B/e)^2$ .

#### IV.1. Conductances in the trivial and topological phases

In this section, we calculate, using Eqs. 17 and 18, the conductance of the coupled system, dot-*sp*-chains in the different topological phases of the chains. When the chains are in the trivial topological phase, i.e., for  $D < 0$  or  $\tilde{V} > 1$ , the conductances are zero at zero temperature, since the chains are insulators, and become finite at finite temperatures due to thermal activation of quasi-particles above the band gap, as shown in Fig. 4. The results presented are obtained for the chemical potential of the chains  $\mu = 0$ , i.e., a full lower band (*half-filling*). The dot energy is given by  $E_0 = 0$  and the coupling between the dot and the chains  $t_d/V_2 = 0.1$ . Fig. 4 also shows the electrical and thermal conductances

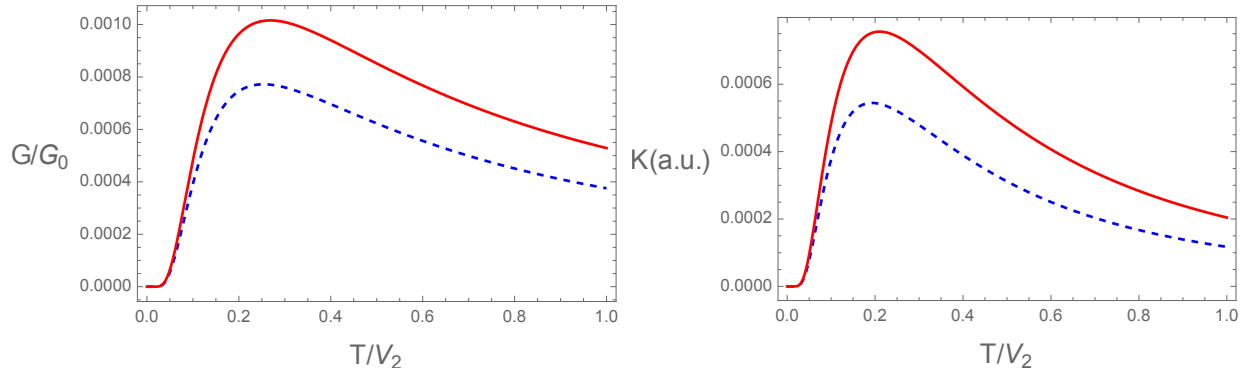


FIG. (4) (Left panel) Dimensionless electrical conductance as functions of temperature in the trivial,  $D = -0.44$  (in red) and topological  $D = 0.36$  (blue dashed line) phases. In all figures shown here the coupling between the dot and the chains is taken as  $t_d/V_2 = 0.1$ . (Right panel) Thermal conductances as functions of temperature in the trivial,  $D = -0.44$  (red solid line) and topological  $D = 0.36$  (blue dashed line) phases.

in the topological phase. They also vanish for  $T = 0$ , as expected, since the *bulk* of the chains is insulating. In Fig. 4

the conductances are obtained for  $D = 0.36$  and  $D = -0.44$ . These values of  $D$  correspond, respectively, to  $\tilde{V} = 0.8$  and  $\tilde{V} = 1.2$ , such that the system is at the same distance but in opposite sides of the topological transition ( $\tilde{V} = 1$ ). We notice that the electrical and thermal conductances are larger in the trivial phase showing that the surface modes can act as scattering centers decreasing the finite temperatures conductances. Besides, the interaction between the surface modes through the dot, shifts the energy of these modes giving rise to an additional gap.

We remark that the thermopower, Eq. 21, cancels out and is zero at all temperatures in both topological and trivial phases due to particle-hole symmetry.

#### IV.2. Conductances at the topological transition

We now obtain the conductances at the topological transition, i.e., at  $D = 0$  or  $\tilde{V} = 1$ . The zero temperature dimensionless electrical conductance in this case is unity showing that a quantum of charge flows through the system. Then, at the transition the surface modes recombine to form a quasi-particle that transports electric current through the dot. The current can flow through the device since at  $D = 0$ , the chains themselves are in a semi-metallic state.

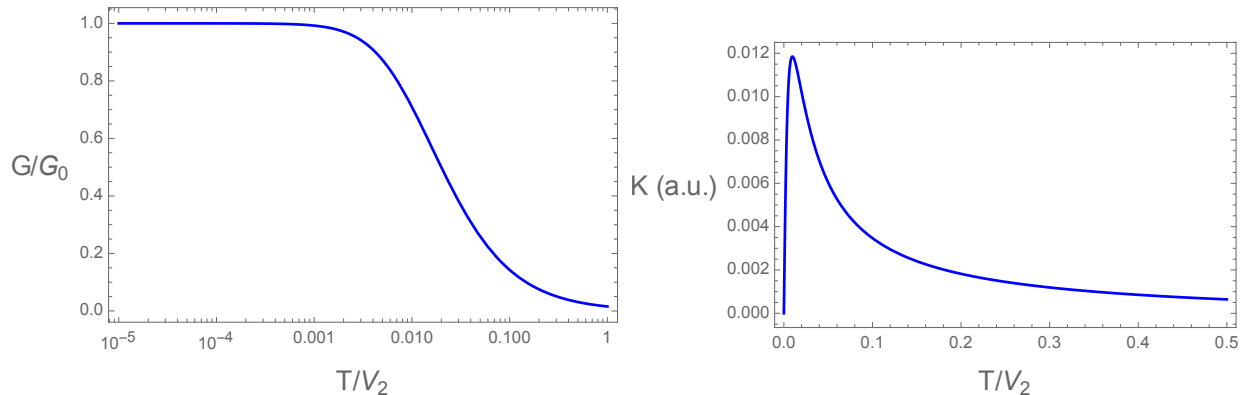


FIG. (5) (Left panel) Dimensionless conductance as a function of temperature at the topological transition,  $V = 1$  or  $D = 0$ . (Right panel) Thermal conductance as a function of temperature at the topological transition,  $D = 0$ . It vanishes at zero temperature differently from the electric conductance.

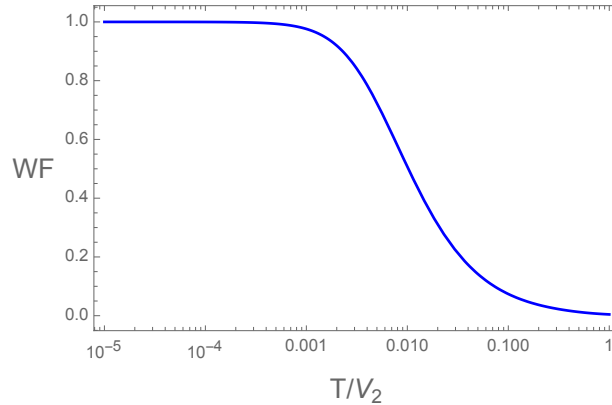


FIG. (6) (Color online) Dimensionless Wiedemann-Franz ratio defined as  $WF = (K/T)_r/(G/G_0)$  as function of temperature at the topological transition. The quantity  $(K/T)_r = (K/T)/(KT)_0$  where  $(KT)_0 = \lim_{T \rightarrow 0} (K/T)$  at the topological transition, i.e., at  $D = 0$ . Notice that the limiting low temperature value of  $(K/T)_r = 1$  here is simply a consequence of the normalization factor.

The zero temperature electrical conductance is universal since it does not depend on the strength ( $t_d$ ) of the coupling of the chains to the quantum dot ( $t_d$ ), as long as the energy of the dot is fixed at  $E_0 = 0$ . The thermal conductance differently from the electrical conductance vanishes at zero temperature, even at the topological transition. It increases and reaches a maximum as temperature increases, as shown in Fig. 5 right panel, before vanishing asymptotically

at high temperatures. Fig. 6 shows the dimensionless Wiedmann-Franz ratio as a function of temperature at the topological transition. It starts as unity at  $T = 0$  and remains constant at this value at very low temperatures. Notice that the unit value at low temperatures is just due to the normalization and is not related to simple metallic behavior. Further on, in Section V.1.3, we shall obtain the Wiedmann-Franz ratio in appropriate units of the Lorenz number  $L_0$ . In the low temperature region  $K/G \propto T$  as in a metal, but this ratio acquires an additional temperature dependence as temperature increases.

We point out that the thermopower, Eq. 21, vanishes at the topological transition since the quantity  $\mathcal{L}_1$  in this equation cancels out due to the equal contributions of electron and holes to the transport properties.

Finally, notice that the results above hold for both types of intra and inter-atomic hybridized *sp*-chains.

## V. THE SP DIATOMIC CHAIN: RICE-MELE MODEL

The *sp*-diatomic chain [19] maps in the Rice-Mele (RM) model [23], which is a generalization of the SSH model that takes into account different local energies for sites in different sub-lattices of the chain. It breaks the chiral symmetry of the original SSH Hamiltonian. The  $k$ -space Hamiltonian of the model can be written in matrix form as

$$H_{RM}(k) = \begin{pmatrix} \epsilon_a - \mu & V_1 + V_2 e^{-ik} \\ V_1 + V_2 e^{ik} & \epsilon_b - \mu \end{pmatrix}$$

where  $\epsilon_{a,b}$  are the local energies in the different sub-lattices and  $\mu$  the chemical potential. The hopping terms  $V_1$  and  $V_2$  are those defined before for the SSH model. We consider, for simplicity, the case  $\epsilon_a = -\epsilon_b = \epsilon$ . The topological phases of the Rice-Mele model can be characterized by Chern numbers [6],  $n_C = -\text{sgn}[\epsilon(V_2 - V_1)]$ , such that for  $V_1 = V_2$  or  $\epsilon = 0$  there are topological quantum phase transitions.

The energy of the bands of the infinite chain are given by

$$\tilde{\omega}_1(k) = -\tilde{\mu} + \sqrt{2\tilde{V} \cos(k) + \tilde{V}^2 + \tilde{\epsilon}^2 + 1} \quad (24)$$

$$\tilde{\omega}_2(k) = -\tilde{\mu} - \sqrt{2\tilde{V} \cos(k) + \tilde{V}^2 + \tilde{\epsilon}^2 + 1} \quad (25)$$

$$(26)$$

The extrema of the bands occur for  $k = \pi$ . Differently from the SSH model there is always a gap between the bands, which is given by

$$\tilde{\Delta} = \tilde{\omega}_1(\pi) - \tilde{\omega}_2(\pi) = 2\sqrt{(1 - \tilde{V})^2 + \tilde{\epsilon}^2}$$

The *tilde* quantities are dimensionless, renormalized by the hopping  $V_2$  and as before,  $\tilde{V} = V_1/V_2$ . Since we will take  $V_2 = 1$ , we will drop the *tilde* from now on.

### V.1. Thermoelectric properties of the diatomic *sp*-chain

#### V.1.1. Electrical conductance

The local Green's function at the edge of the semi-infinite diatomic *sp*-chain is obtained from the self-consistent equation,

$$G_{00}(\omega) = \begin{pmatrix} \omega + \mu - \epsilon & V_1 & 0 \\ V_1 & \omega + \mu + \epsilon & V_2 \\ 0 & V_2 & G_{00}^{-1} \end{pmatrix}_{(00)}^{-1}. \quad (27)$$

As before, we can obtain the surface density of states of the semi-infinite diatomic *sp*-chain or semi-infinite Rice-Mele model. This is given by,

$$\begin{aligned} \rho(\omega) = & \left| 1 - \tilde{V}^2 \right| \delta(\mu + \omega - \epsilon) + \left( 1 - \tilde{V}^2 \right) \delta(\mu + \omega - \epsilon) + \\ & \frac{\text{sgn}(\mu + \omega) \Im m \left( \sqrt{\left( -(\mu + \omega)^2 + (1 - \tilde{V})^2 + \epsilon^2 \right) \left( -(\mu + \omega)^2 + (1 + \tilde{V})^2 + \epsilon^2 \right)} \right)}{2(\mu + \omega - \epsilon)} \end{aligned} \quad (28)$$

Notice the presence of a surface mode, now at a finite energy  $\omega_S = \epsilon - \mu$ , in the case  $\tilde{V} < 1$ . Differently from the SSH model, at  $\tilde{V} = 1$  there is no gap closing and the system is always gapped. However, the phases of the Rice-Mele model with  $\tilde{V} > 1$  and  $\tilde{V} < 1$  can still be distinguished by their Chern numbers, as we pointed out before.

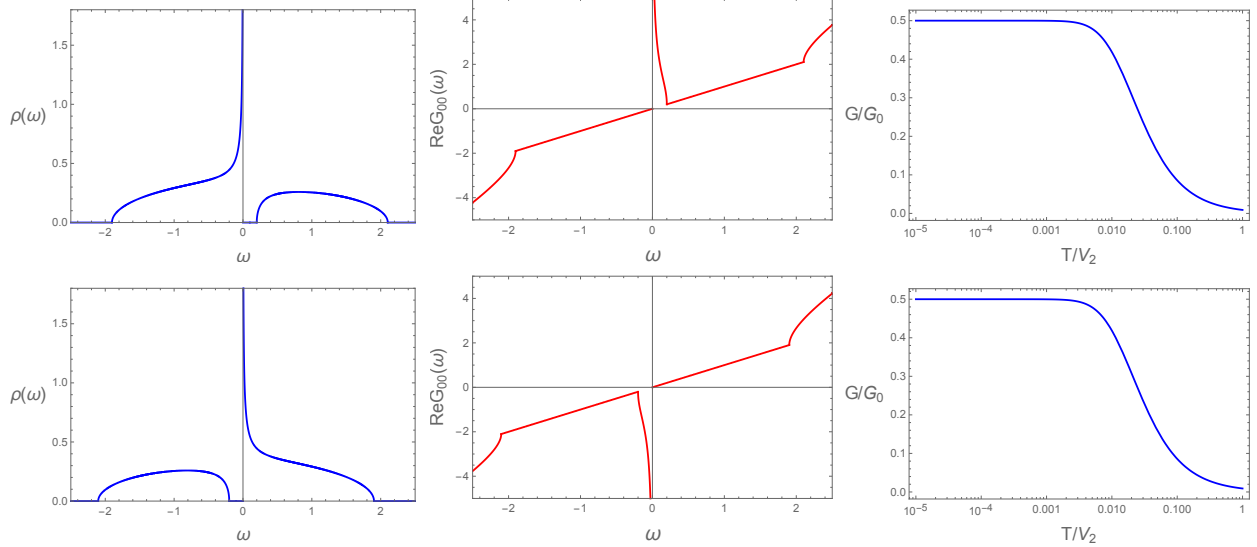


FIG. (7) (Left panel) Surface density of states of the semi-infinite diatomic sp-chain (RM chain), Eq. 28, at the topological transition ( $\tilde{V} = 1$ ), for  $\epsilon = \pm 0.1$  (lower and upper figures, respectively). The chemical potential is on top of the energy of the local modes in both cases ( $\mu = \epsilon$ ). (Middle panel) Real part of the surface Green's function for the same values of  $\epsilon$  and  $\mu$  and  $\tilde{V} = 1$  of the left panel. (Right panel) Normalized conductances as functions of temperature at the topological transition  $\tilde{V} = 1$ . For all panels the coupling dot-chains  $t_d/V_2 = 0.1$ . The energy of the dot  $E_0$  is such that it is always in resonance with the zero mode.

Fig 7 shows the surface density of states, the real part of the surface Green's function and the electrical conductance of a quantum dot attached to two-semi-infinite diatomic *sp* or RM-chains, at the topological transition  $\tilde{V} = 1$ . The figures are for two values of the energy of the local surface mode,  $\epsilon = \pm 0.1$ . The chemical potential is located on the energies of these modes ( $\mu = \epsilon$ ). The energy  $E_0$  of the dot is fixed by the condition that it is always in resonance with the zero mode. The zero energy modes coincide with the top or bottom of the valence and conduction bands. This implies that these are delocalized modes that extend throughout the whole system. The normalized conductance at zero temperature at  $\tilde{V} = 1$  now attains a universal value of 1/2, expected when the edge excitations have fractional charges. These fractional charges are a direct consequence of the breaking of chiral symmetry of the original SSH model, due to the finite and distinct energies of the sub-lattice sites of the Rice-Mele model.

Away from the topological transition the conductance is thermally activated for both phases (not shown).

### V.1.2. Thermopower

The thermopower is a unique and interesting physical property that contains fundamental information on both, transport and thermodynamic properties of the system. The temperature dependence of the thermopower of the device consisting of two diatomic *sp*-chains coupled to the quantum dot can be obtained using Eq. 21. At the topological transition ( $V_1 = V_2$ ), this is shown in Fig. 9 for  $\mu = \epsilon$  and the cases of  $\epsilon$  positive and negative. The corresponding surface density of states for these two cases is shown in the left panel of Fig. 7. The thermopower is either positive or negative depending whether the charge carriers occupying the zero mode is a hole or a particle, respectively. The thermopower is constant at low temperatures and its absolute value decreases with increasing temperature. It is remarkable that it does not vanish as  $T \rightarrow 0$  as expected from the third law of thermodynamics. This is a consequence of the degeneracy of the zero mode [24], as we discuss below. Mathematically, it arises since the function  $\mathcal{T}(\omega)$  in Eq. 19 has a jump discontinuity and is non-differentiable at  $\omega = 0$ , which precludes a low temperature Sommerfeld expansion.

For a gas of charged particles, the thermopower is the entropy per carrier divided by the charge of the carrier [25],

$$S_0 = \frac{\text{entropy per carrier}}{q^*}.$$

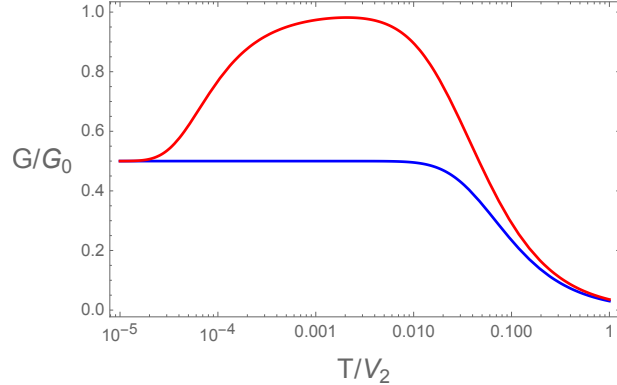


FIG. (8) (Color online) Normalized conductances as a function of temperature at the topological phase transition of the diatomic *sp*-chain for two values of the ratio  $\epsilon/t_d$ . In blue  $\epsilon/t_d = 0.67$ , and in red  $\epsilon/t_d = 3.3 \times 10^{-4}$ . The low temperature saturation value  $G/G_0 = 1/2$  value give evidence of the fractional charge of the quasi-particles in the system. These curves for  $G/G_0$  are independent of the sign of  $\epsilon$ , for  $\mu = \epsilon$  and the dot in resonance with the zero mode. Notice that for small values of  $\epsilon/t_d$  and finite temperatures there is a kind of recombination of the fractional charges.

The entropy per carrier is  $S = \ln 2$  and remains finite at  $T = 0$  due to the double degeneracy of the zero mode [24], i.e, whether it is occupied by a particle or by a hole. These are the current carriers at the topological transition. For a gas of fermions with fractional charge,  $q^* = \pm 1/2$  (in units of electric charge), we get

$$S_0 = \frac{\ln 2}{(\pm 1/2)} = \pm 2 \ln 2 \approx \pm 1.386(k_B/e)$$

These are the low temperature saturation values, obtained numerically for the thermopower using Eq. 21, as shown in Fig. 9. They are expressed only in terms of fundamental constants. These results corroborate the existence of carriers with fractional charges in the diatomic *sp*-chain as already indicated by the electrical conductance at the topological transition. Then, at this transition the electrical carriers occupying the zero mode state have fractional charges,  $q = \pm e/2$ . This is not unexpected considering the mapping of the diatomic *sp*-chain in the Rice-Mele model and what is known about this latter system [23].

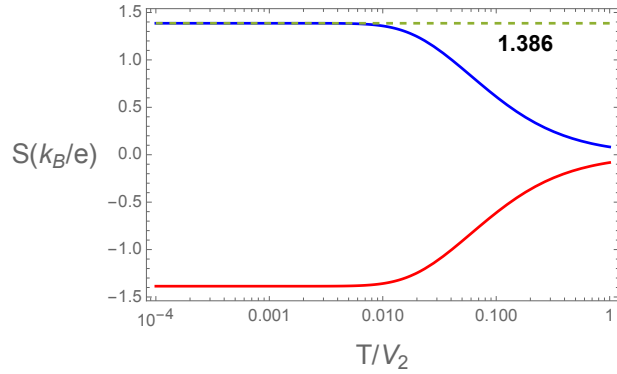


FIG. (9) (Color online) Thermopower as a function of temperature in units of  $(k_B/e)$  at the topological phase transition of the diatomic *sp*-chain. In blue  $\mu = \epsilon = +0.1$ , and in red  $\mu = \epsilon = -0.1$ . The low temperature saturation values correspond to  $S_0 = \pm 2 \ln 2 \approx \pm 1.38634$ , as discussed in the text. They give evidence of the fractional charge of the quasi-particles,  $q^* = \pm e/2$ . The thermopower does not vanish and approaches  $S_0$  as  $T \rightarrow 0$  since the zero energy mode is doubly degenerate.

### V.1.3. Thermal conductance and Wiedemann ratio

The thermal conductance divided by temperature ( $K/T$ ) at the topological transition of the diatomic  $sp$ -chain is shown in Fig. 10. Using the results for the thermopower and Eq. 20, we can determine the limiting value  $(K/T)_0 = (K/T)_{T \rightarrow 0}$ . We find a universal value given by,

$$(K/T)_0 = \frac{\pi^2}{6} - \frac{1}{2}(2 \ln 2)^2 \approx 0.684, \quad (29)$$

in excellent agreement with the numerical results shown in Fig. 10. The Wiedemann-Franz ratio at the topological

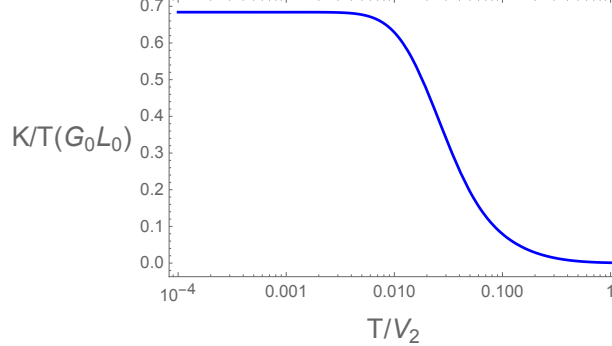


FIG. (10) Thermal conductance of the  $sp$ -diatomic chain divided by temperature at the topological transition in units of  $G_0 L_0$ , where  $L_0$  is the Lorenz number. The zero temperature limiting value  $(K/T)_0 \approx 0.684$ .

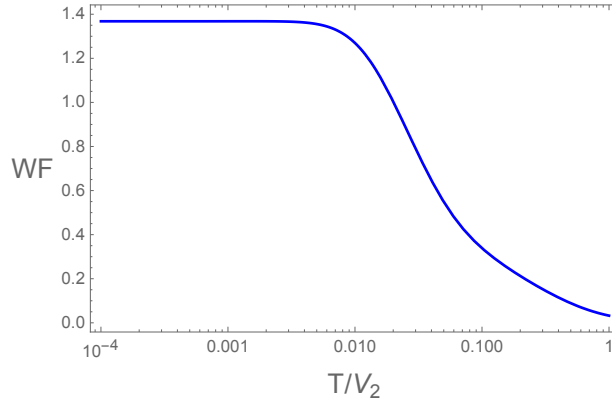


FIG. (11) Wiedemann-Franz ratio of the of the  $sp$ -diatomic chain at the topological transition as function of temperature in units of  $L_0$ . The parameters are the same of Fig. 7, WF is also universal, independent of the values of  $\mu$  and  $\epsilon$  as long as,  $\mu = \epsilon$ .

transition of the diatomic  $sp$ -chain is shown in Fig. 11. Its limiting value is also universal,  $WF(T \rightarrow 0) = 2(K/T)_0 = (\pi^2/3) - (2 \ln 2)^2 \approx 1.368$  in units of  $L_0$ , as long as the dot is in resonance with the zero energy mode. This value of WF is different from that of a simple metal where  $WF = 1$  (in units of  $L_0$ ), besides it is a function of temperature and vanishes asymptotically for large temperatures.

## V.2. Figure of merit and power factor

Fig. 12 shows the dimensionless figure of merit  $ZT = (S^2 GT)/K$  and power factor at the topological transition as functions of temperature. The latter is defined as  $PF = (\widetilde{PF}/S_0^2 G_0)$ , where  $S_0$  is the zero temperature thermopower and  $G_0$  the unit of conductance. The quantity  $\widetilde{PF} = S^2 G$  is the full dimensional power factor [26]. These quantities ZT and PF do not depend on the sign of  $\epsilon$  but only on its absolute value. Notice that the figure of merit ZT has a

maximum ( $ZT_{max} \approx 1.6$ ) at sufficiently high temperatures since the energy scale  $V_2$  is of the order of a bandwidth ( $\sim 1$  eV). The power factor is still important at the temperature of this maximum in ZT. The significance of the former is that, in a time reversible system at steady state, the maximum power for conversion of heat into work is given by  $P_{max} = (1/4)\widetilde{PF}$  for two heat reservoirs with a difference in temperature  $\Delta T = 1$  K. The efficiency of a device at this maximum power is given by [26],

$$\eta(P_{max}) = \frac{\eta_C}{2} \frac{ZT}{ZT + 2}$$

where  $\eta_C$  is the efficiency of a Carnot engine working between the same reservoirs. The efficiency of our device at  $ZT_{max}$  turns out to be  $\eta \approx \eta_C/5$ .

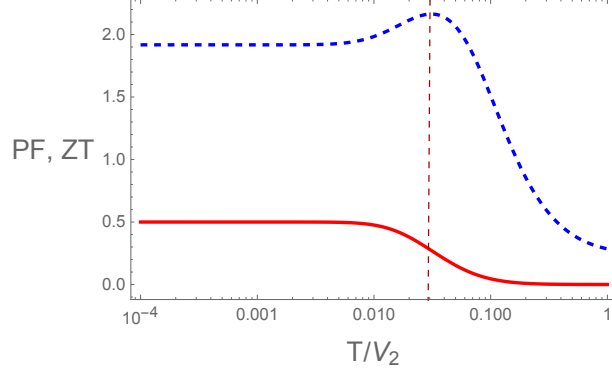


FIG. (12) (Color online) Dimensionless figure of merit ZT (blue dashed line) and dimensionless power factor PF (red solid line) as functions of temperature for  $\epsilon = \mu = \pm 0.1$ . These curves depend only on the absolute value of  $\epsilon$ .

## VI. CONCLUSIONS AND PERSPECTIVES

The study of topological materials is a recent and important research area in condensed matter physics. These systems in their topological phase present protected surface modes that opens the possibility of several applications. In particular in the case of  $p$ -wave topological superconducting chains, the edge modes are emergent Majorana fermions, which attract a lot of attention. However,  $p$ -wave superconductors occur only scarcely in nature and the quest for Majoranas poses huge experimental challenges.

Topological insulating chains are simpler systems with also very exciting properties. These chains can be realized in materials with hybridized  $sp$ -states where the anti-symmetric nature of the hybridization between orbitals of different parities guarantees their topological properties. We consider in this work two types of  $sp$ -chains where the  $sp$  hybridization is either intra-atomic, or interatomic. We also studied  $sp$  diatomic chains. In the former two cases the  $sp$ -chains map in the well studied SSH chain and in the latter in the Rice-Mele problem. We study the topological properties of these chains directly through the *surface* density of states at the edge of a semi-infinite chain. We show that in both types of mono-atomic  $sp$ -chains there are genuine topological surface states whose weights vanish continuously when approaching the transition from the topological to the trivial phase. In the inter-atomic  $sp$ -chain, the surface state is known to be a hybrid quasi-particle with  $s$  and  $p$  character.

In order to study the transport properties of the  $sp$ -chains, we considered a simple device consisting of a quantum dot connected to two identical semi-infinite  $sp$ -chains. At the topological transition and zero temperature, the conductance in the case of monoatomic chains takes the universal value  $G/G_0 = 1$ , since the surface modes penetrate into the bulk and the system carries current even at  $T = 0$ . The universal behavior of the conductance reflects the topological nature of the end states in the semi-infinite chains. The normalized Wiedemann-Franz ratio is obtained and we find that the thermal conductivity vanishes at  $T = 0$  even at the topological transition. Away from the topological transition and  $T = 0$ , the current through the device vanishes as expected, since the wires are insulators, whether they are topologically trivial or not. However, at finite temperatures there is activated transport that as we have shown is different in the trivial and topological phases.

An interesting behavior arises when we extend the model for a diatomic chain with different sub-lattices local energies. In this case the finite local energies break the chiral symmetry of the SSH Hamiltonian and the chain is now modeled by the Rice-Mele Hamiltonian. This system still presents non-trivial topological phases that are now

characterized by Chern numbers. Interestingly, the zero temperature dimensionless conductance at the topological transition assumes the value  $G/G_0 = 1/2$ , as would be expected for carriers with fractional charges. In this case, as pointed out above, this is a direct consequence of the breakdown of the chiral symmetry of the original SSH model. The thermopower is extremely interesting in these chains, since it does vanish at zero temperature and gives direct information on the (fractional) charges of the carriers.

Away from the topological transition, either in the trivial or non-trivial phases the transport properties of the insulating chains are thermally activated. However, at the fine tuned transition there is charge transport even at  $T = 0$ , as we have shown. In this case it is interesting to compare the physical properties of the fractional charge carriers in the topological insulators with those of Majorana modes in  $p$ -wave superconductors [27].

The  $sp$ -chains, with edge modes in their topological phases, are interesting materials, easier to realize in practice than  $p$ -wave superconductors. They are potentially useful systems exhibiting properties that can be explored in a large temperature range.

## VII. ACKNOWLEDGMENTS

MAC acknowledges the Brazilian agency CNPq, and Fundação de Amparo a Pesquisa do Estado do Rio de Janeiro FAPERJ for partial financial support.

---

[1] J. Alicea, Reports on Progress in Physics **75**, 076501 (2012).  
 [2] S. Rachel, Reports on Progress in Physics **81**, 116501 (2018).  
 [3] A. Y. Kitaev, Physics-Uspekhi **44**, 131 (2001).  
 [4] E. Vernek, P. H. Penteado, A. C. Seridonio, and J. C. Egues, Phys. Rev. B **89**, 165314 (2014).  
 [5] T. Mizushima, Y. Tsutsumi, M. Sato, and K. Machida, Journal of Physics: Condensed Matter **27**, 113203 (2015).  
 [6] S.-Q. Shen, *Springer Series in Solid-State Sciences 187 Topological Insulators Dirac Equation in Condensed Matter Second Edition*, Springer Series in Solid-State Sciences, Vol. 187 (Springer Singapore, Singapore, 2017).  
 [7] M. Z. Hasan and C. L. Kane, Rev. Mod. Phys. **82**, 3045 (2010), arXiv:1002.3895.  
 [8] M. A. Continentino, H. Caldas, D. Nozadze, and N. Trivedi, Phys. Lett. Sect. A Gen. At. Solid State Phys. **378**, 3340 (2014), arXiv:1405.4183.  
 [9] K. Sun, W. V. Liu, A. Hemmerich, and S. Das Sarma, Nature Physics **8**, 67 (2012).  
 [10] W. P. Su, J. R. Schrieffer, and A. J. Heeger, Phys. Rev. B **22**, 2099 (1980).  
 [11] W. A. Chalifoux and R. R. Tykwinski, Nature Chemistry **2**, 967 (2010).  
 [12] V. I. Artyukhov, M. Liu, and B. I. Yakobson, Nano Letters, Nano Letters **14**, 4224 (2014).  
 [13] B. Pan, J. Xiao, J. Li, P. Liu, C. Wang, and G. Yang, Science Advances **138**, 1106 (2015).  
 [14] Q. Sun, L. Cai, S. Wang, R. Widmer, H. Ju, J. Zhu, L. Li, Y. He, P. Ruffieux, R. Fasel, and W. Xu, Journal of the American Chemical Society **138**, 1106 (2016).  
 [15] L. Shi, P. Rohringer, K. Suenaga, Y. Niimi, J. Kotakoski, J. C. Meyer, H. Peterlik, M. Wanko, S. Cahangirov, A. Rubio, Z. J. Lapin, L. Novotny, P. Ayala, and T. Pichler, Nature Materials **15**, 634 (2016).  
 [16] E.-N. Foo and H.-S. Wong, Phys. Rev. B **9**, 1857 (1974).  
 [17] H. Caldas, R. L. S. Farias, and M. Continentino, Phys. Rev. A **88**, 023615 (2013).  
 [18] E. N. Foo and L. G. Johnson, Surf. Sci. **55**, 189 (1976).  
 [19] E.-N. Foo and D. Giangiulio, Phys. B+C **84**, 167 (1976).  
 [20] E.-N. Foo, M. Thorpe, and D. Weaire, Surface Science **57**, 323 (1976).  
 [21] M. M. Odashima, B. G. Prado, and E. Vernek, Rev. Bras. Ensino Física **39**, 1 (2016), arXiv:1604.02499.  
 [22] L. S. Ricco, F. A. Dessotti, I. A. Shelykh, M. S. Figueira, and A. C. Seridonio, Sci. Rep. **8**, 2790 (2018).  
 [23] M. J. Rice and E. J. Mele, Phys. Rev. Lett. **49**, 1455 (1982).  
 [24] S. N. Kempkes, A. Quelle, and C. M. Smith, Scientific Reports **6**, 38530 (2016).  
 [25] P. M. Chaikin, “An introduction to thermopower for those who might want to use it to study organic conductors and superconductors,” in *Organic Superconductivity*, edited by V. Z. Kresin and W. A. Little (Springer US, Boston, MA, 1990) pp. 101–115.  
 [26] G. Benenti, G. Casati, K. Saito, and R. S. Whitney, Physics Reports **694**, 1 (2017).  
 [27] G. W. Semenoff and P. Sodano, Journal of Physics B: Atomic, Molecular and Optical Physics **40**, 1479 (2007).